Simulation and Analysis of the LZ Amplifier and Cables

Jyothisraj Johnson[1]
Advisors: Prof. Mani Tripathi[2], Seth Hillbrand[2]

[1]CUNY: Hunter College
[2]University of California, Davis

Abstract

After development of a model for pure voltage SPHE signals, a systematic analysis of the current design of the LZ amplifier was undertaken. Furthermore, a model for the current pulse created at the output of the PMTs in response to a SPHE was derived and a simulation of the coaxial cable and feedthrough connector that this pulse propagates through was developed in order to realistically model more components of the LZ data acquisition chain.

1 Introduction

1.1 Dark Matter

Both strong and weak gravitational lensing, in addition to rotational curves of galaxies, have provided indirect evidence for the existence of dark matter on a large scale throughout the universe. Much of these indirect observations have come from observing its gravitational effects. Galaxies near the Milky Way rotate faster than their visible matter should allow for. In the case of strong gravitational lenses, the observed multiple images sometimes have anomalies in either their positions or fluxes that can be explained by invisible clumps of matter, or in other words, dark matter nearby the images [4]. There are many candidates for dark matter particles including sterile neutrinos, axions and WIMPs. The LUX-Zeppelin (LZ) experiment seeks to directly detect WIMPs interacting with ordinary matter.

1.2 The LZ Experiment

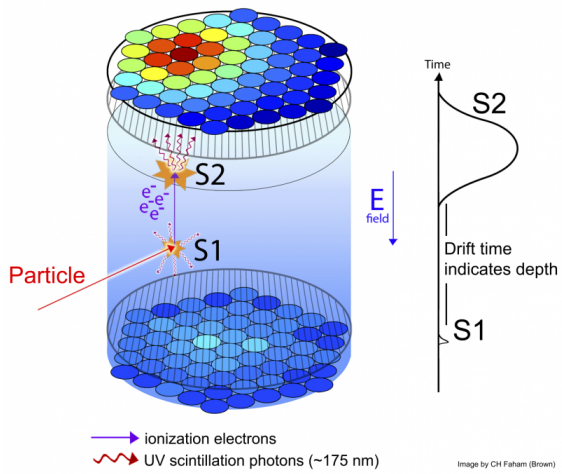

Figure 1: Diagram showing the TPC of the LZ experiment (Credit: CH Faham, Brown University)

LZ is a dual phase time projection chamber experiment (see Figure 1) [3]. The dual phase characterization comes from Xenon existing in two states, liquid and gas, inside of the chamber. Liquid Xenon is used because it is inert, thus it is easy to purify, and it is very low in radioisotopes, thus it naturally has a low radioactive background [2].

Furthermore, it has a relatively high Z value and because interaction cross section scales with Z^2, there is a higher chance of WIMP interactions [2]. The experiment's classification as a time projection experiment is because an accurate location for every particle interaction within the chamber can be calculated. When particles, mostly neutrons and electrons, collide with the liquid Xenon in the chamber, they release primary scintillation (S1) signals. They also ionize the liquid Xenon and free electrons, which are then accelerated upwards into the top of the chamber with an applied external electric field. Once there, freed electrons interact with the gaseous Xenon present and produce a secondary scintillation (S2) signal. An array of photomultiplier tubes is located at the top and bottom of the TPC (see Figure 2). Calculating a ratio of total signal received by each PMT allows for an accurate calculation of the (x,y) location of the particle interaction within the chamber. Calculating the time delay between the PMTs detecting the S1 and S2 signals allows us to determine the depth of the initial interaction within the TPC. Thus, an accurate 3D location of the particle interaction can be established [1]. The ratio of the area of the S2/S1 signals plotted against the recoil energy allows for classification of interactions and eliminates certain interactions as WIMP candidate events [1].

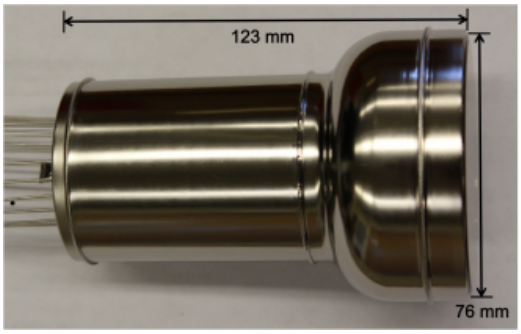

Figure 2: A Hamamatsu R11410-20 PMT, the type that will be used for LZ (Credit: Lung et. al. 2012).

1.3 The LZ Data Acquisition Chain

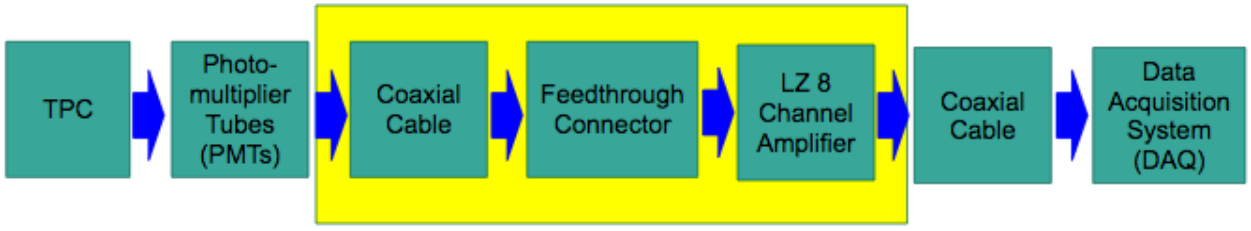

Figure 3: My summer project focused on the part of the signal chain highlighted in yellow.

The LZ experiment data acquisition chain is not as simple as digitizing and recording the signal as it leaves the PMTs. The current pulses at the PMTs' output are too sharp and small to be digitized properly. Thus, the signal must pass through a coaxial cable and feedthrough cable that brings the signal to the input of the LZ amplifier, where it is optimally shaped and amplified before passing through another coaxial cable and reaching the DAQ systems for digitization (see Figure 3 above) [3]. My summer project focused on the propagation of signal from the PMTs to the LZ amplifier and the shaping and amplification of the signal as it travels through the amplifier itself. One of two goals for the project was to construct a cable simulation of the signal from leaving the PMTs as a current pulse to reaching the input of the amplifier as a voltage signal across a termination resistor. The other was to conduct a systematic analysis of the LZ amplifier itself to make sure specifications are met. We used transient, noise and gain/phase analyses, which are the industry standard.

2 Simulations

2.1 The SPHE Current Pulse Model for Cable Simulations

For the cable simulations, we wanted to model the current pulse produced at the output of the PMTs in response to a single photoelectron (SPHE), which is the electron emitted from an atom after an interaction with a photon via the photoelectric effect. The SPHE is excited at the photocathode of a PMT. We know the ideal gain of the PMT across the 12 dynodes. Using this gain factor, we calculated the average value of a current pulse that lasts eight nanoseconds and calculated the total area of the expected pulse in units of μA*ns. We decided to use a triangle wave to model the current pulse and thus, for a calculated area of 320μA*ns, our model has an amplitude of 40μA, rise time of 6ns and fall time of 10ns (see Figure 4).

2.2 Constructing a Cable Simulation

One unfamiliar with signal propagation analysis might not understand the need for cable simulations in the first place. Internal components of coaxial cables, such as the inner conductor, shielding, and general specifications of the cable produce varying levels of signal attenuation and deformation (see Figure 5). The LZ experiment requires that we fully understand this attenuation of signal and ensure that it doesn't hinder the goals of the experiment. In general, these factors that affect the signal are referred to as parasitics. A coaxial cable's parasitics include the self-capacitance and self-inductance as well as the total resistance of the cable, which primarily depends on the inner conductor material. In addition, there is a frequency dependent resistance of the cable shielding that is on the order of mΩ/m at low frequencies but is on the order of Ω/m at the frequencies we deal with: ~100-300MHz.

Figure 4: Input SPHE current pulse for the cable simulations. Peak: 40uA, Rise: 6ns, Fall: 10ns

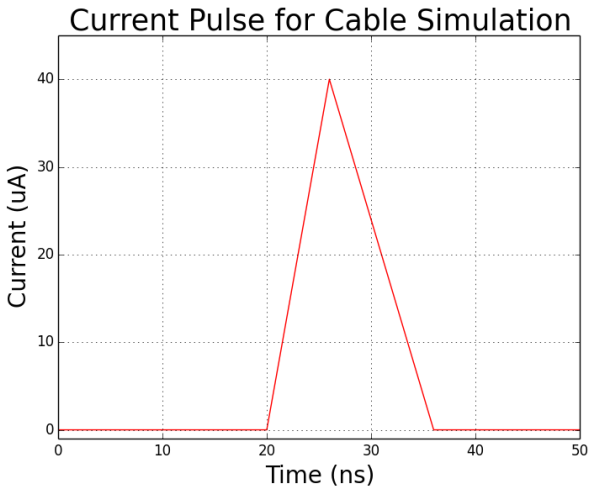

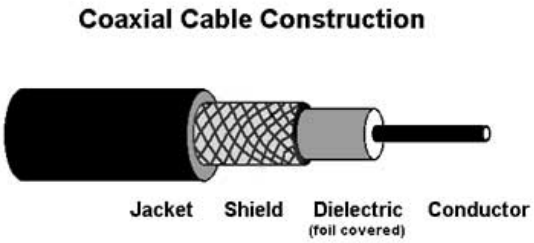

Figure 5:Image shows inner components of coaxial cable (Credit: The Fiber Optic Assoc., Inc)

On top of simulating the parasitics of the cable, we also calculated the parasitics of the feedthrough connector, a DB-25 connector. The connector has parasitics in the form of pin-pin capacitance and contact resistance.

A decision on the specific coaxial cable and DB-25 connector that will be used for the final design of the LZ data acquisition chain has not been

made. In lieu of this, we looked online at the cable data sheets that GORE, a private cable manufacturer that was used for the LUX experiment, provided on their website and similarly, we considered a range of DB-25 connectors from different manufacturers. We looked into how widely the parasitics differed and chose appropriate values. A table of parasitics and the appropriate values we used for our simulation based on data sheets and/or calculations is listed below (see Table 1). As we can see, the parasitics of the DB-25 connector are negligible but those of the cable are not.

Table 1: List of the different parasitics considered and their respective values per feet; total cable length was 45ft.

Parasitic	Value
DB-25 Pin-Pin Capacitance	0.12pF
DB-25 Contact Resistance	10mΩ
Cable Capacitance	19.4pF/ft
Cable Resistance	0.22Ω/ft
Cable Inductance	0.441μH/ft

2.3 The Three Iterations of the Cable Simulation

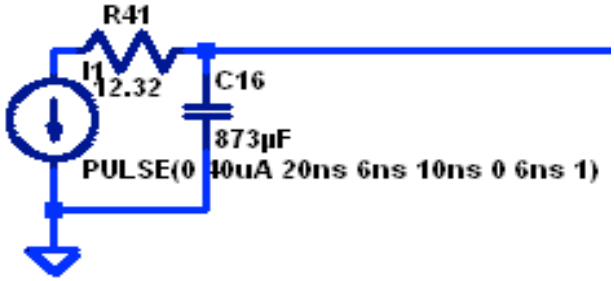

Figure 6: Initial cable simulation using only 1 RC filter to model waveform propagation.

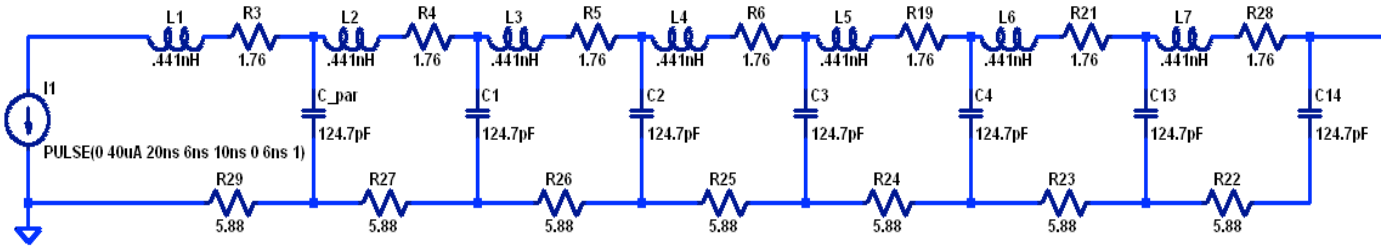

Figure 7: Cable simulation using 7 LRCs to model waveform propagation.

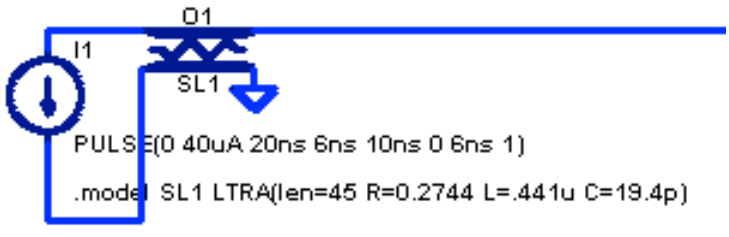

Figure 8: Cable simulation using a Lossy Transmission Line model (LTRA), which consists of a very large array of LRCs to model waveform propagation.

When starting to model the cable simulation, we decided to start from a very basic and simple model and build up as necessary. We compared the output of the cable simulation to the experimental

outputs one of the LUX/LZ collaborators had plotted. The amplitude of the voltage pulse was not required to match as that was highly dependent on the termination resistance. The full width half maximum (FWHM) and full width tenth maximum (FWTM) were our primary points of comparison as they remain the same independent of voltage amplitude at mV scales. Our first attempt at a model was a simple RC low pass filter as shown in Figure 6. This filter modeled the total resistance and capacitance of the cable but did not include the inductance of the cable. We wanted to see if it was necessary to model the inductance. The tail of the output of this simulation was extremely long and the amplitude was so small (on the order of 10μV's) that the output was in essence a DC line. This model turned out to be highly unrealistic due to the fact that the signal sees an extremely large capacitance of the total cable length at once instead of spread out infinitesimally as should be the case. This resulted in an extremely wide FWTM and FWHM so the model was immediately discounted. In our next cable simulation model, we used a row of 7 LRCs to model the inductance, resistance and capacitance as well as high frequency impedance of the cable shielding; the model is shown in Figure 7. As we can see in Figure 9, the output of this model has a long tail present and the FWTM is larger by an approximate factor of six but the FWHM is comparable. In our third cable simulation model that we tested, we used a built in LTSpice model: The Lossy Transmission Line (LTRA) model (see Figure 8). This doesn't take into account the high frequency impedance of the cable shielding but models waveform propagation as a very large array of LRCs that represent infinitesimal sections of the total cable length. The model takes as its inputs the total cable length, and the resistance, inductance and capacitance per unit length. The output of this cable simulation is shown in Figure 10. Both the FWTM and FWHM are within 10% of our collaborator's plots. Although, I was not able to finalize a cable simulation during my ten weeks in the program, we are now fairly close to accurately and realistically simulating signal propagation through a coaxial cable. This is tremendously useful as we can input the specified parameters of various cables that we are considering using for the final LZ design and see the effects it will have on signal deformation and attenuation without having to buy all the various types of cables and experimentally test all of them ourselves.

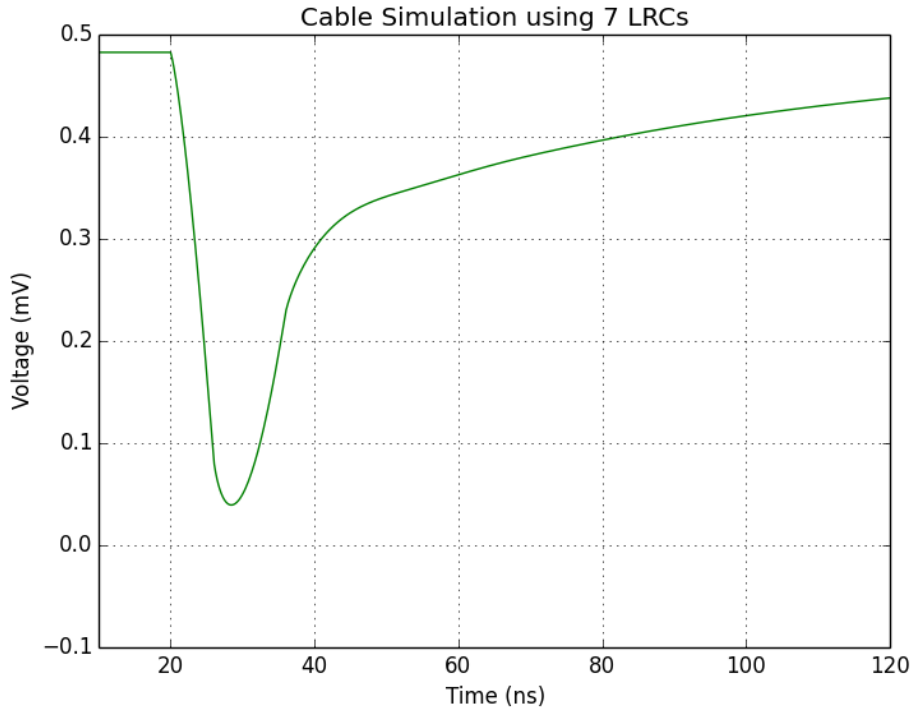

Figure 9: Output voltage pulse of the 7 LRC cable simulation. FWHM: 11.3ns, FWTM: 99.45ns

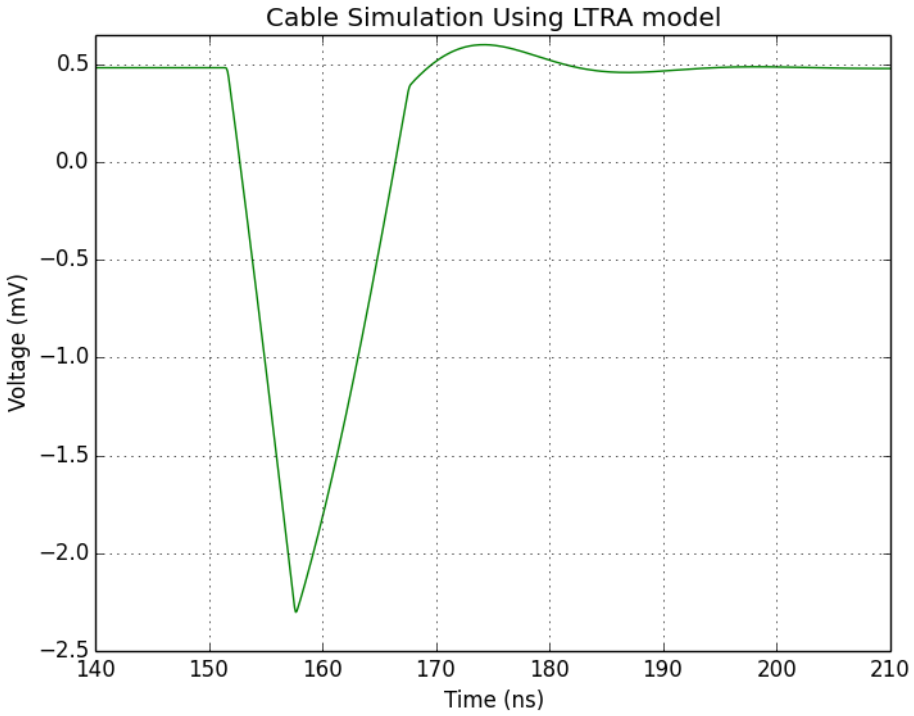

Figure 10: Output voltage pulse of the infinitesimal LRC segments cable simulation. FWHM: 8.62ns, FWTM: 14.71ns

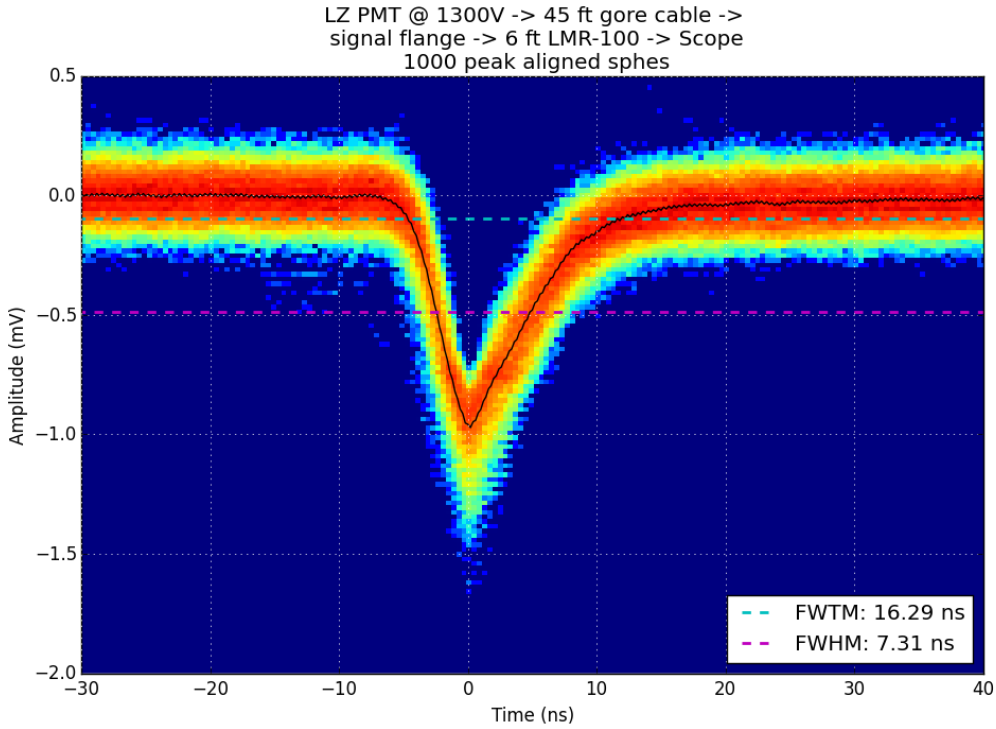

Figure 11: Experimental results of 1000 peak aligned SPHEs with FWHM and FWTM shown

3 Conducting a Systematic Analysis of the LZ Amplifier

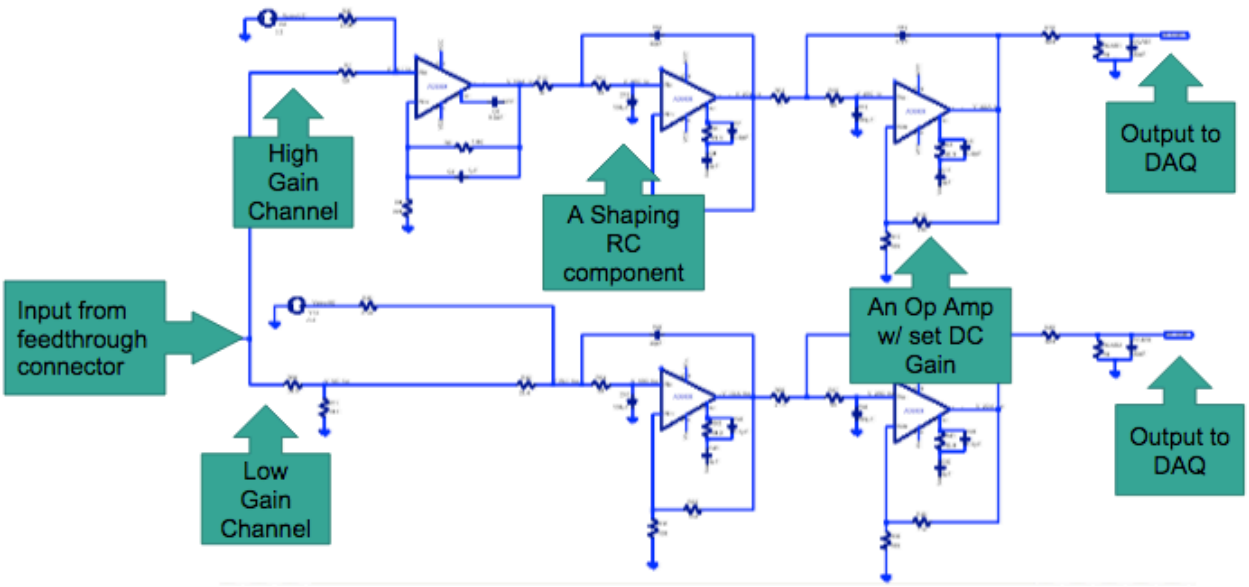

Figure 12: The current design of the LZ amplifier circuit, with the high gain channel on top and low gain on the bottom.

Before moving on to the general design of the LZ amplifier itself, it is important to discuss a crucial component that not everyone might be familiar with. Operational Amplifiers (Op Amps) are fundamentally differential voltage amplifiers. They amplify the difference in the voltage between the two inputs by a gain factor on the order of 10^6. This extremely high open loop gain is not stable as small environmental factors, such as temperature, can cause relatively large changes to this gain. In order to stabilize and control the DC gain of the amplifier, a negative feedback loop is introduced as shown in Figure 13. This sets the DC gain of this configuration of resistors as (1+Rf/Rg) and it is the primary configuration used in the LZ amplifier design.

Figure 12 shows the propagation of the signal through the two channel amplifier. RC circuits are used as shaping circuits that attenuate the signal amplitude but widen the signal range, which is required for optimal digital reconstruction of the signal at the analog-digital converter in DAQ. There are high gain and low gain channels to deal with the variety of signals that are shaped and amplified by this circuit. We would not want to amplify and shape a SPHE waveform that passes through this circuit in the same way we deal with a comparatively very high energy S2 signal. Thus, to deal with extrema at both

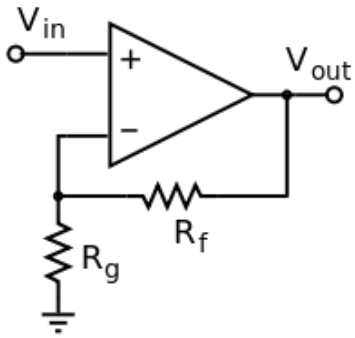

Figure 13: Shown is a diagram of an Op Amp using resistors to set its DC gain (Credit: Wikipedia)

ends of the energy spectrum, we have two channels that provide an optimal dynamic range for the circuit.

The second goal of the summer project was to conduct a systematic analysis of the LZ amplifier. We used three industry standard analyses: transient, noise and gain/phase analyses.

Transient analysis is a crucial type of analysis built into LTSpice that allows us to accurately predict what happens to the input signal as it propagates through the circuit at every node in the circuit. Below we can see this for ourselves in Figures 14-17. The

benefit of knowing this is making sure the output from the two channels is optimal for digitization in DAQ. The digitizer samples every ten nanoseconds so the signal needs to be sufficiently spread out and amplified so that signal shape and amplitude can be preserved during the digitization process.

Every internal component in any circuit has noise in some form. This includes but is not limited to resistors, capacitors, and op amps. This noise is amplified along with the signal at the various op amps in the LZ amplifier design. Conducting a noise analysis allows for the calculation of the one sigma standard deviation from zero of the noise amplitude. This is very important because we need to maintain a S/N ratio so that we can distinguish between signal in the form of SPHE and noise. High noise in the circuit inhibits this ability.

In Figure 18, the output of the high gain channel noise analysis is shown. Frequency is shown on the x-axis and the square root of the power density is shown on the y-axis in terms of nV/√(Hz). Using a plot like this, we can calculate the one sigma standard deviation from zero of noise signals' amplitude at a specific frequency. For example, if we pick 10^6 Hz as our frequency of choice, we would take the square root of this frequency and multiply that by the square root power density value at that frequency to obtain the one sigma standard deviation from zero. In this case, that value is 0.14mV. The three sigma standard deviation is then 0.42mV. Expected amplitudes of SPHE voltage pulses tend to be between 0.7mV and 1.3mV (see Figure 11). Thus in this case, we will be able to distinguish between signal and noise sufficiently well.

The third type of systematic analysis that I conducted is gain/phase analysis. This serves an important function of understanding the gain at every node of the LZ amplifier but most importantly at the output and making sure it matches specifications. We can also make sure that we prevent ringing, or self-oscillations, within the circuit. If the gain, in dB, is positive while the phase is 180°, there will be ringing introduced at that frequency. I have shown the output of the high gain channel gain/phase analysis in Figure 19. As shown, the condition for self-oscillations is met at $2*10^7$ Hz, where the phase is 180° out of phase and there is a gain of 33dB. It is rare to see signals of this frequency during normal operation of the LZ experiment however so this is not an immediate cause for concern. However, the significance of these analysis is that we are able to see these results beforehand and anticipate problems before they occur and without having to build and experimentally test every version of the amplifier.

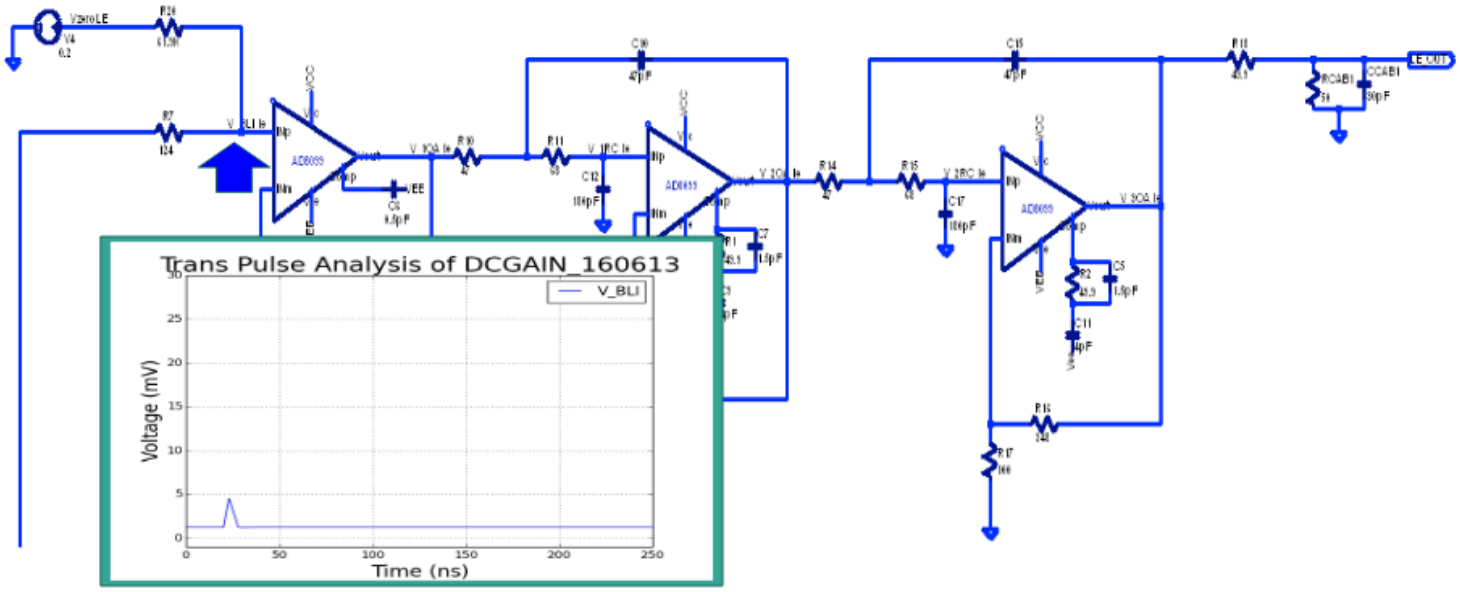

Figure 14: The input SPHE voltage pulse shown before propagation through the high gain channel of the amplifier

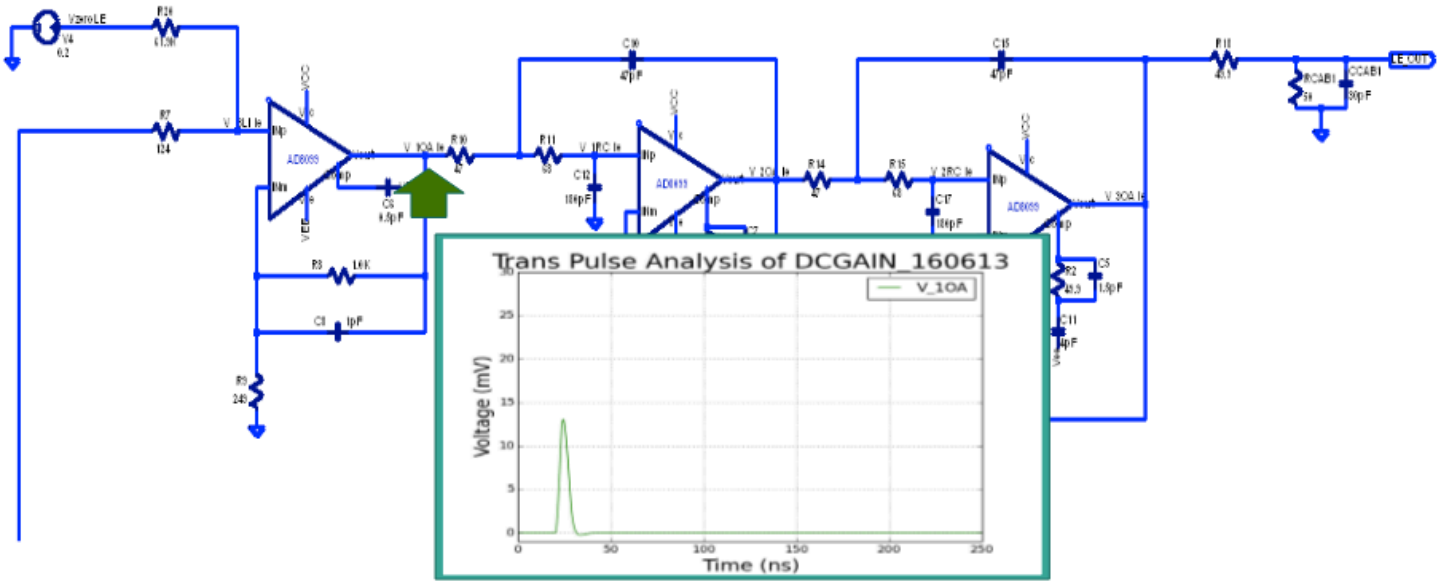

Figure 15: Input SPHE signal after passing through first op amp of the high gain channel of the LZ amplifier

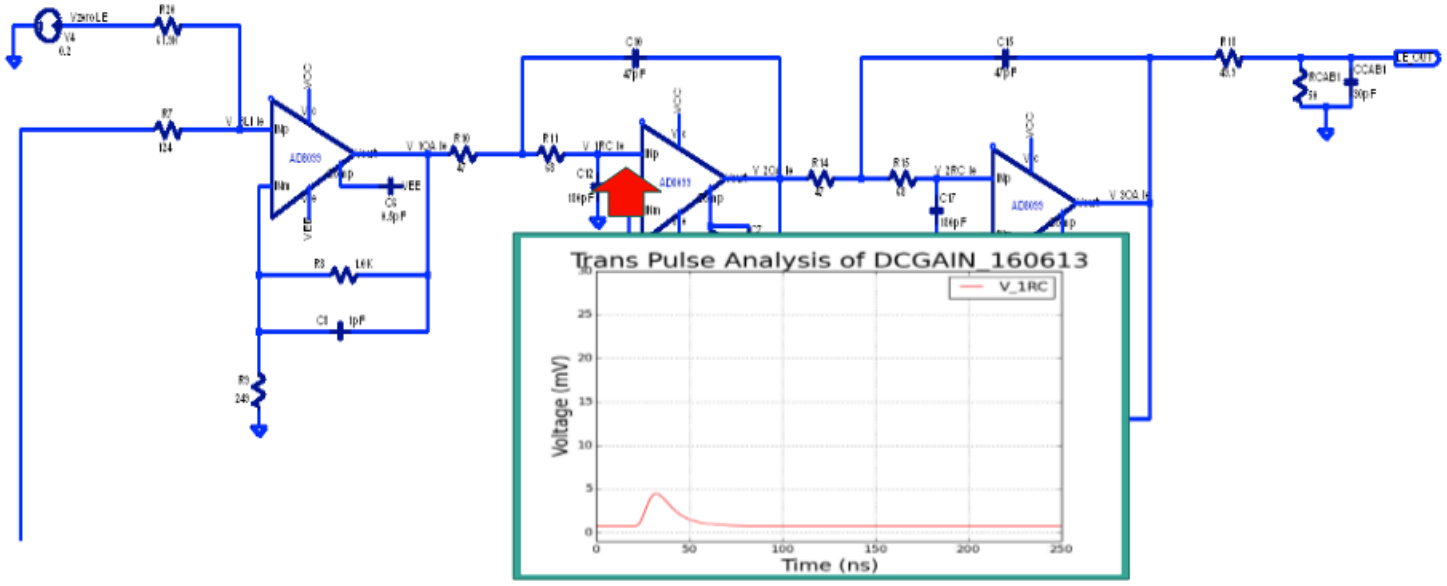

Figure 16: Input SPHE signal after passing through first RC filter of the high gain channel of the LZ amplifier

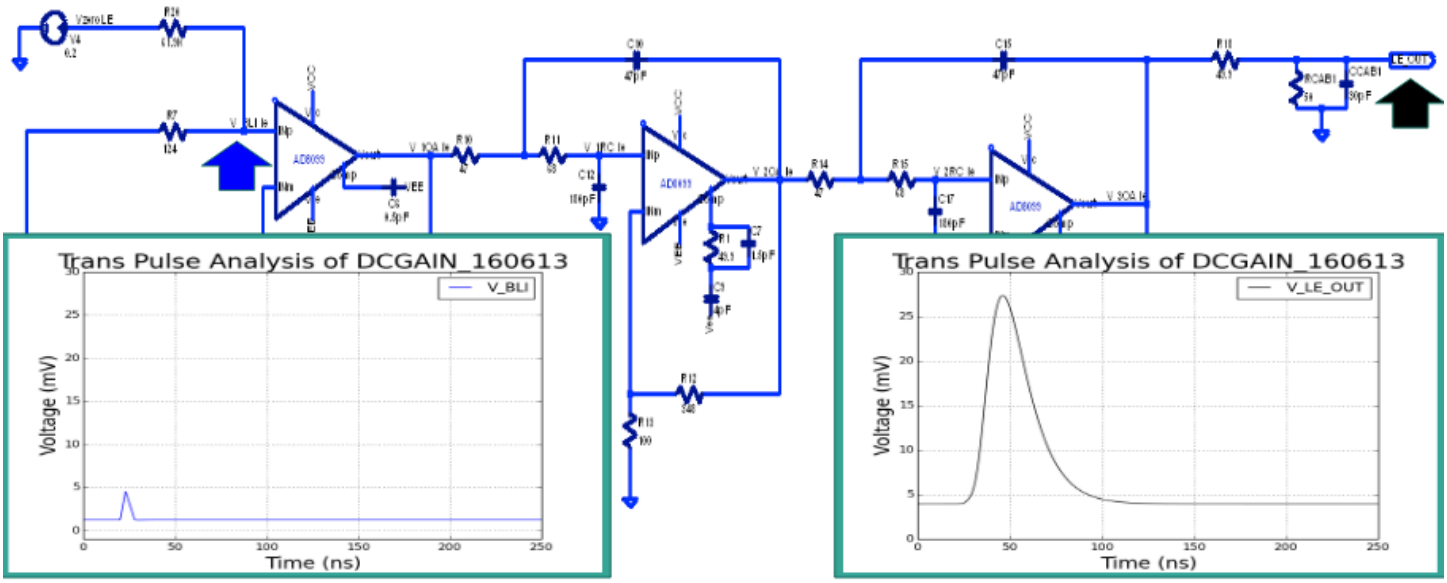

Figure 17: Input SPHE signal before and after passing through the whole high gain channel of the LZ amplifier

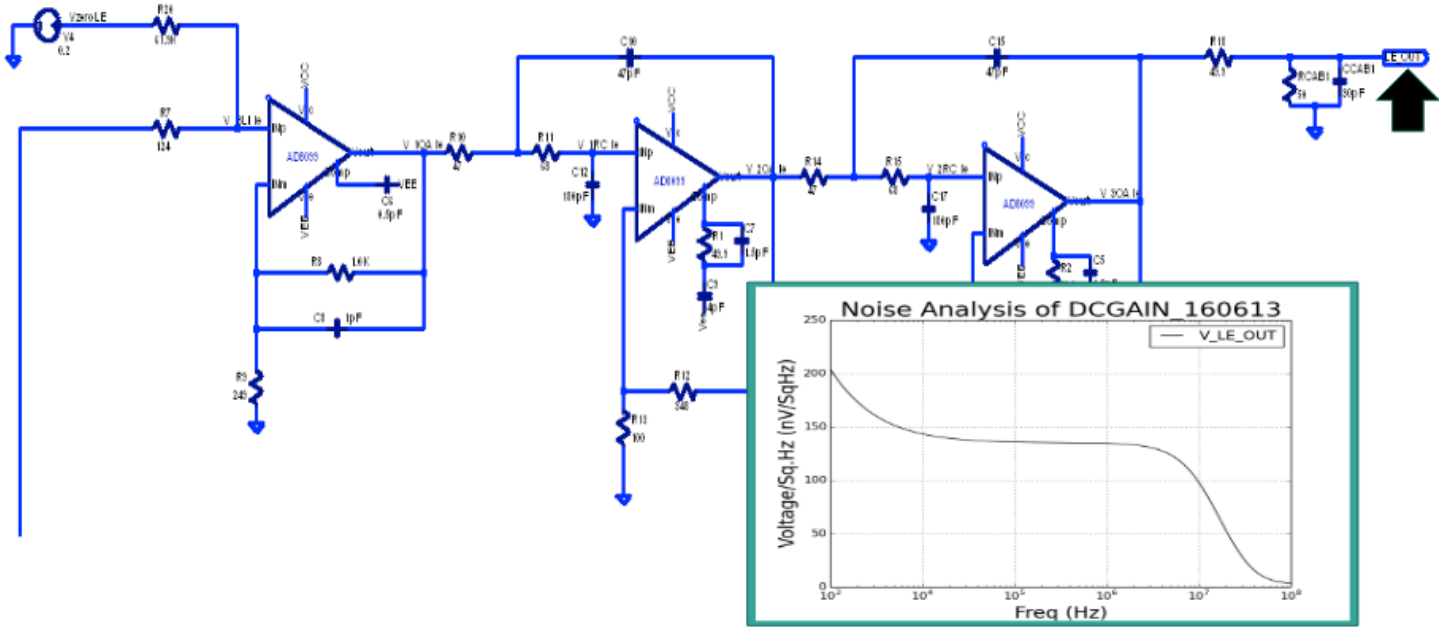

Figure 18: Noise analysis plot at the output of the high gain channel of the LZ amplifier

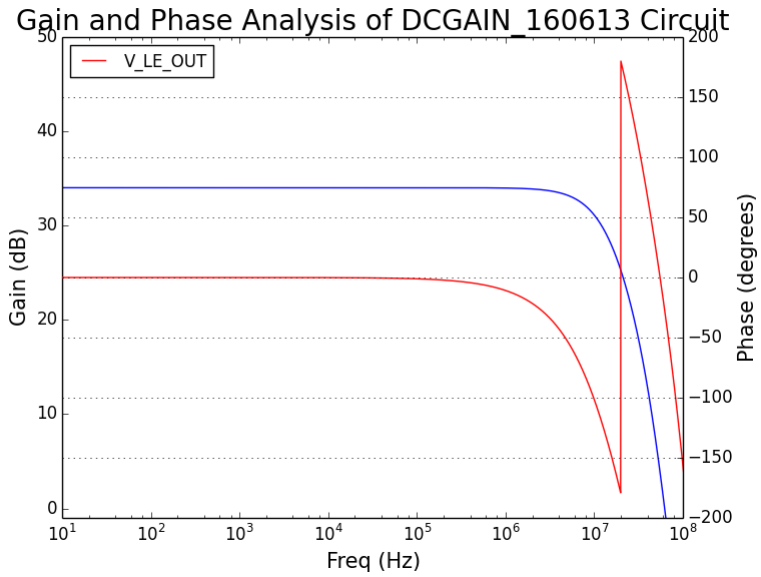

Figure 19: The LZ amplifier high gain channel output of the Gain/Phase analysis plot

4 Conclusion

In conclusion, after development of a model for pure voltage S2 and SPHE signals, a systematic analysis of the current design of the LZ amplifier was undertaken. This was done to understand and characterize the output signal of the amplifier as well as its noise at various frequency ranges. We wanted to maintain high S/N ratios at all frequencies and know which frequencies are prone to self-oscillations due to its positive gain and 180° phase difference between input and output voltage pulses. A model for the current pulse at the output of the PMTs in response to a SPHE was derived. Using this waveform, we simulated the coaxial cable and feedthrough connector that this pulse propagates through. The simulation was conducted in order to realistically model more components of the LZ data acquisition chain.

In the future, a finalized model of signal propagation from the output of the PMTs to the input of DAQ will be used to test each updated version of the amplifier to make sure signal shaping and amplification matches specifications. We can also save money by not having to test various cables using experimental set ups if we have an accurate and realistic simulation whose parameters can be updated to reflect specific cables from different manufacturers. Furthermore, setting up an experiment for and creating a database of SPHE signals leaving the PMTs will allow us to have a more realistic input to use for our cable and LZ amplifier simulations.

References

[1] D. S. Akerib, X. Bai, S. Bedikian, E. Bernard, A. Bernstein, A. Bolozdynya, A. Bradley, D. Byram, S. B. Cahn, C. Camp, et al. The large underground Xenon (LUX) experiment. Nuclear Inst. and Methods in Physics Research, A704 (2013) 111 – 126, 2012

[2] M. Schumann. Dual-Phase Liquid Xenon Detectors for Dark Matter Searches. JINST 9 C08004, 2014

[3] D. S. Akerib, C. W. Akerlof, D. Yu. Akimov, S. K. Alsum, H. M. Araújo, X. Bai, A. J. Bailey, J. Balajthy, S. Balashov, M. J. Barry, P. Bauer, et al. LUX-ZEPLIN (LZ) Conceptual Design Report. arXiv:1509.02910, 2015

[4] Wambsganss, J. Gravitational Lensing in Astronomy. Living Rev. Relativity 1, 1998